Nuclear Instruments and Methods in Physics Research B 114 (1996) 237–244

NIM B
Beam Interactions with Materials & Atoms

ELSEVIER

Brilliance of coherent peaks for type-B photoproduction of electron–positron pairs in a crystal

Yu.P. Kunashenko [a,*], Yu.L. Pivovarov [b]

[a] *Institute of Physics, University of Trondheim, Norway*

[b] *Nuclear Physics Institute, P.O. Box 25, 634050 Tomsk, Russian Federation*

Received 14 October 1994; revised form received 13 July 1995

Abstract

The shape and magnitude of coherent peaks are studied for the type-B coherent photoproduction of electron–positron pairs in a crystal, in the energy range of photons $\omega = 10^2$–10^3 MeV. It is shown that under detection of pairs with restricted emission angles the coherent peaks (as a function of photon energy ω) become more brilliant, with larger value of relation of peak height to background, and lower width. The influence of channeling effect on the position of coherent maxima is estimated.

1. Introduction

The type-A coherent creation of e^+e^- pairs by the high energy photons in a crystals has been predicted [1,2] and experimentally observed for the total pair yield [3]. The type-A coherent processes in a crystal take place when the angle between the photon momentum and the crystal axis is quite large. During the last years the interest in the coherent pair photoproduction in the crystals is connected with the coherent process of type-B, when the photon momentum is parallel to the crystal axis. In this case the coherent maxima arise at a sufficiently lower photon energies as compared with the type-A coherent photoproduction.

The type-B coherent pair photoproduction in a crystal has been predicted in Refs. [4,5] and experimentally observed in Ref. [6] for the total yield of pairs (integrated over particles energies and emission angles) in a crystal C⟨100⟩ for the photon energies from 100 MeV to 1 GeV, and in Ref. [7] for the yield of symmetrical pairs in Ge⟨111⟩ and Si⟨100⟩ crystals for photon energies range 100–550 MeV. The observed enhancement of the yield due to coherence effect was about 10–20%, both for detection of all emitted pairs [6] and for detection of only symmetrical pairs [7]. The goal of this paper is to show how the detection of the created particles with definite kinematical characteristics increases sufficiently (in terms of orders of magnitude) the relation between the coherent peak and the incoherent background.

2. Theory

The cross-section of e^+e^- pair creation in a crystal can be expressed as usual [1–5] by the sum of coherent $d\sigma_{coh}$ and incoherent $d\sigma_{incoh}$ parts:

$$d\sigma = d\sigma_{coh} + d\sigma_{incoh}. \tag{1}$$

For a type-B process (the photon momentum $\boldsymbol{k}$ is parallel to the crystal axis OZ) in the separate string approximation (simple estimations show, that the separate string approximation is valid when an angle between photon momentum and crystal string is smaller than d_{st}/L, where d_{st} is distance between the crystals neighboring strings and L is the thickness of a crystal)

$$\frac{d\sigma_{coh}}{d\Omega_+\, d\Omega_-\, d\varepsilon_+} = \frac{d\sigma_1}{d\Omega_+\, d\Omega_-\, d\varepsilon_+} \exp(-q^2\bar{u}^2)|S(q_\parallel)|^2 \times \left|\sum_{n=0}^{N-1} \exp(iq_\parallel nd)\right|^2,$$

$$\frac{d\sigma_{incoh}}{d\Omega_+\, d\Omega_-\, d\varepsilon_+} = \frac{d\sigma_1}{d\Omega_+\, d\Omega_-\, d\varepsilon_+} N\left[1 - \exp(-q^2\bar{u}^2)\right]. \tag{2}$$

Here the units $\hbar = c = 1$ are used, $d\sigma_1/d\Omega_+\, d\Omega_-\, d\varepsilon_+$ is the pair photoproduction cross-section on a separate atom of a crystal, $\varepsilon_+(\varepsilon_-)$ and $\boldsymbol{p}^+(\boldsymbol{p})$ are the positron (electron) energy and momenta, $d\Omega_+(d\Omega_-)$ is the elementary solid angle, $\exp(-q^2\bar{u}^2)$ is the Debye–Waller factor taking into account the thermal vibrations of the crystal atoms,

* Corresponding author. On leave from Nuclear Physics Institute, P.O. Box 25, 634050 Tomsk, Russian Federation.

SSDI 0168-583X(95)01261-3

$$\boldsymbol{q} = \boldsymbol{k} - \boldsymbol{p}^+ - \boldsymbol{p}^- = \boldsymbol{q}_\parallel + \boldsymbol{q}_\perp,$$

is the momentum transferred with $\boldsymbol{q}_\perp$ is perpendicular to $\boldsymbol{k}$, and $\boldsymbol{q}_\parallel$ is parallel to $\boldsymbol{k}$, $S(\boldsymbol{q}_\parallel)$ is the structure factor of the crystal axis and N is the number of atoms in an axis, with d being the crystal lattice constant, and

$$I(q_\parallel) = \left|\sum_{n=0}^{N-1} \exp(iq_\parallel nd)\right|^2 = \frac{\sin^2(Nq_\parallel d/2)}{\sin^2(q_\parallel d/2)}, \tag{3}$$

being the interference multiplyer. As it follows from Eqs. (2)–(3), the coherent contribution to the cross-section has the sharp maxima (coherent peaks) at

$$q_\parallel = \omega - p_\parallel^+ - p_\parallel^- = g_n, \quad n = 1, 2, 3, \ldots, \tag{4}$$

where $\omega = k$ is the photon energy, $p_\parallel^\pm$ is the projection of electron (positron) momentum on the crystal axis, $g_n = g_0 n$ ($g_0 = 2\pi/d$) is the reciprocal lattice vector. In the relativistic limit ($\omega \gg m$) the emission angles of electron and positron are small: $\Theta_\pm \sim m/\omega \ll 1$, and the relation (4) takes the form:

$$\omega - p^+(1 - \Theta_+^2/2) - p^-(1 - \Theta_-^2/2) = g_n,$$
$$n = 1, 2, 3, \ldots . \tag{5}$$

As it follows from Eq. (5), if $\mathrm{d}\sigma_1/\mathrm{d}\Omega_+\,\mathrm{d}\Omega_-\,\mathrm{d}\varepsilon_+ \neq 0$, then for every fixed momenta of the electron p^- and the positron p^+ one can find those values of ω, Θ_+, Θ_- (or for fixed $p^+\Theta_+$ one can find the necessary ω and $p^-\Theta_-$, etc.) when the interference multiplyer equals N^2 and the cross-section has a sharp peak.

Let us start with the analysis of coherent type- B effect in a thin crystal. It is useful to know the formula for the differential over angles Θ_+ and Θ_- cross-section and integrated over an angle φ between the momenta of electron and positron in a plane perpendicular to the initial photon momentum. After substitution of the differential cross-section of pair photoproduction from Ref. [12] into Eq. (2) one has

$$\frac{\mathrm{d}\sigma_{\mathrm{coh}}}{\xi_+\,\mathrm{d}\xi_+\xi_-\,\mathrm{d}\xi_-\,\mathrm{d}\varphi\,\mathrm{d}x} = \sigma_0 \frac{\Xi(\xi_-, \xi_+, \varphi)}{\left[Q^2(\xi_-, \xi_+, \varphi) + (\lambda/R)^2\right]^2} \times \exp(-q^2\bar{u}^2)\left|S(q_\parallel)\right|^2 \left|\sum_{n=0}^{N-1} \exp(iq_\parallel nd)\right|^2;$$

$$\frac{\mathrm{d}\sigma_{\mathrm{incoh}}}{\xi_+\,\mathrm{d}\xi_+\xi_-\,\mathrm{d}\xi_-\,\mathrm{d}\varphi\,\mathrm{d}x} = N\sigma_0 \frac{\Xi(\xi_-, \xi_+, \varphi)}{\left[Q^2(\xi_-, \xi_+, \varphi) + (\lambda/R)^2\right]^2}\left[1 - \exp(-q^2\bar{u}^2)\right];$$

here $\lambda = \hbar/mc = 1/m$ is the electron Compton wavelength, $r_0 = e^2/mc^2 = e^2/m$ is the classical electron radius, $\alpha = e^2/\hbar c = e^2$ is the fine structure constant, $x = \varepsilon_+/\omega$, $\xi = \Theta_\pm/\omega$, $\gamma = \varepsilon_\pm/m$. We took into account the atomic screening in the form $V(r) = (Ze/r)\exp(-r/R)$ and introduced the notations:

$$\sigma_0 = \frac{8}{\pi}\frac{\varepsilon_+\varepsilon_-}{\omega^2} Z^2\alpha r_0^2 = \frac{8}{\pi} x(1-x) Z^2 \alpha r_0^2,$$

$$\Xi(\xi_-, \xi_+, \varphi) = -\frac{\xi_+^2}{(1+\xi_+^2)^2} - \frac{\xi_-^2}{(1+\xi_-^2)^2} + \frac{1}{2x(1-x)}\frac{\xi_+^2 + \xi_-^2}{(1+\xi_+^2)(1+\xi_-^2)} + \left(\frac{x}{1-x} + \frac{1-x}{x}\right)\frac{\xi_+\xi_-\cos\varphi}{(1+\xi_+^2)(1+\xi_-^2)}, \tag{6}$$

$$Q^2(\xi_-, \xi_+, \varphi) = \xi_+^2 + \xi_-^2 + 2\xi_+\xi_-\cos\varphi + \left(\frac{m}{2\omega}\right)^2\left[\frac{1+\xi_+^2}{x} + \frac{1+\xi_-^2}{1-x}\right]^2, \tag{7}$$

Since the function

$$F(\varphi) = \frac{1}{\left[Q^2(\xi_-, \xi_+, \varphi) + (\lambda/R)^2\right]^2}, \tag{8}$$

has a very sharp maximum at $\varphi \simeq \pi$:

$$F(\varphi) \sim \begin{cases} \gamma^4 \gg 1; & \gamma \gg (R/\lambda) \\ (R/\lambda)^4 \gg 1; & \gamma \ll (R/\lambda), \\ (\gamma^2 + (\lambda/R)^2)^{-2} \gg 1; & \gamma \sim (R/\lambda), \end{cases} \tag{9}$$

(for photon energy of order of hundreds of MeV, $F(\pi) \sim 10^8$–10^9), and

$$F(0) \sim F(2\pi) \sim 1, \qquad \xi_\pm \sim 1,$$

and the remaining multiplyers in Eqs. (5) and (6) are slowly changing functions of φ, we keep only $F(\varphi)$ under the integral sign and take the remaining factors at $\varphi = \pi$. After the integration we found:

$$\frac{\mathrm{d}\sigma_{\mathrm{coh}}}{\xi_+\,\mathrm{d}\xi_+\xi_-\,\mathrm{d}\xi_-\,\mathrm{d}x} = \sigma_0\Xi(\xi_-, \xi_+, \pi)E(\xi_-, \xi_+, \pi)\Phi(\xi_-, \xi_+) \times \left|S(q_\parallel)\right|^2 \left|\sum_{n=0}^{N-1} \exp(iq_\parallel nd)\right|^2, \tag{10}$$

$$\frac{\mathrm{d}\sigma_{\mathrm{incoh}}}{\xi_+\,\mathrm{d}\xi_+\xi_-\,\mathrm{d}\xi_-\,\mathrm{d}x} = \sigma_0 N\Xi(\xi_-, \xi_+, \pi)\,(1 - E(\xi_-, \xi_+, \pi))\,\Phi(\xi_-, \xi_+), \tag{11}$$

where

$$\Phi(\xi_-,\xi_+) = \frac{2\pi/a^2}{(1-b^2/a^2)^{3/2}}; \tag{12}$$

$$a = a(\xi_-,\xi_+) = \xi_+^2 + \xi_-^2 + \left(\frac{m}{2\omega}\right)^2 \left[\frac{1+\xi_+^2}{x} + \frac{1+\xi_-^2}{(1-x)}\right]^2 + (\lambda/R)^2, \tag{13}$$

$$b = b(\xi_-,\xi_+) = 2\xi_+\xi_-, \tag{14}$$

$$E(\xi_-,\xi_+,\varphi) = \exp\left[-Q^2(\xi_-,\xi_+,\varphi)\bar{u}^2m^2\right]. \tag{15}$$

The cross-section for e^+e^- pair photoproduction on N atoms in an amorphous target one can find by substitution $\bar{u}^2 = \infty$ into formulae (10) and (11):

$$\frac{d\sigma_N}{\xi_+\, d\xi_+ \xi_-\, d\xi_-\, dx} = \sigma_0 N \Xi(\xi_-,\xi_+,\pi)\Phi(\xi_-,\xi_+). \tag{16}$$

The obtained Eqs. (10), (11) and (16) are used in numerical calculations below in Section 3.

It is obvious that the measurement of any differential cross-section under the condition (5) can lead to an observation of the sharp coherent peaks. In a real experiment, due to angular and energy resolutions of a detecting system, one can only approach the exact condition (5) and the sharp maxima will be "washed away". Moreover, the large crystal thickness usually used in an experiments allows to substitute the interferential multiplyer $I(q_\parallel)$ given by Eq. (3) by the sum of δ-functions

$$I(q_\parallel) = \frac{\sin^2(\frac{1}{2}Nq_\parallel d)}{\sin^2(\frac{1}{2}q_\parallel d)} = g_0 N \sum_{n=-\infty}^{n=\infty} \delta(q_\parallel - g_0 n).$$

One of the simplest ways to measure the pair yield with given kinematical characteristics, could be the detection of pairs with the fixed value of x, emitted at angles less than the chosen Θ_m (some kind of the collimation, or momenta correlation).

The pair yield with fixed energies of electron ε_- and positron ε_+, into the emission angle cone $\Theta_\pm \le \Theta_m$, with Δ the angle between the crystal axis and the axis of emission cone, one can calculate by substitution of the differential cross-section from Ref. [12] into Eq. (2) and integration over permitted emission angles.

Taking into account Eq. (4) and

$$p^{(\pm)} = \left(\varepsilon_\pm^2 - m^2\right)^{1/2} \simeq \varepsilon_\pm\left(1 - 1/2\gamma_\pm^2\right),$$

we rewrite further $\delta(q_\parallel - g_0 n)$ in the form:

$$\delta(q_\parallel - g_0 n) = \delta\left[\frac{\varepsilon_+}{2\gamma_+^2}(\xi_+^2+1) + \frac{\varepsilon_-}{2\gamma_-^2}(\xi_-^2-1) - ng_0\right] = \frac{2\gamma_+^2}{\varepsilon_+}\delta\left\{\xi_+^2 - \left[\frac{2\gamma_+^2 n g_0}{\varepsilon_+} - \zeta(\xi_-^2-1)\right]\right\},$$

where $\zeta = \gamma_+/\gamma_- = \varepsilon_+/\varepsilon_- = x/(1-x)$. Now the integration over ξ_+ is trivial due to δ-functions and we immediately obtain:

$$\frac{d\sigma_{coh}}{dx} = N\pi\sigma_0\gamma_+\frac{\lambda}{d}\int_{-\varphi_0}^{\varphi_0} d\varphi \int_{(\Delta\gamma_-)^2}^{((\Delta+\Theta_m)\gamma_-)^2} d\xi_-^2 \sum_{n=n_1}^{n_2} \frac{\Xi(\xi_-,\xi_n,\varphi)E(\xi_-,\xi_n,\varphi)}{\left[Q^2(\xi_-,\xi_n,\varphi) + (\lambda/R)^2\right]^2}\left|S(q_\parallel)\right|^2. \tag{17}$$

Here, Δ is the angle between the crystal axis and the axis of solid angle over which the integration is performed; Θ_m, φ_0 define the integration region.

The functions $\Xi(\xi_-,\xi_n,\varphi)$, $Q^2(\xi_-,\xi_n,\varphi)$ and (ξ_-,ξ_n,φ) in the Eq. (17) are obtained from Eqs. (6), (7) and (15) by substitution $\xi_+ \longrightarrow \xi_n$, where

$$\xi_n = \frac{4\pi\gamma_+\lambda}{d}n - 1 - \zeta(1+\xi_-^2); \tag{18}$$

and n_1, n_2 define the reciprocal lattice vectors which give rise to the cross-section for the given photon energy and permitted region of the emission angles for electron and positron. For our kinematics,

$$n_1 = \frac{d}{4\pi\gamma_+\lambda}\left[\gamma_+^2\Delta^2 + 1 + \zeta(1+\xi_-^2)\right],$$

$$n_2 = \frac{d}{4\pi\gamma_+\lambda}\left[\gamma_+^2(\Delta+\Theta_m)^2 + 1 + \zeta(1+\xi_-^2)\right].$$

The incoherent part (the same notations used) has the form:

$$\frac{d\sigma_{incoh}}{dx} = N\sigma_0 \int_{-\varphi_0}^{\varphi_0} d\varphi \int_{(\Delta\gamma_-)^2}^{((\Delta+\Theta_m\gamma_-)^2} \frac{1}{2}\, d\xi_-^2 \int_{(\Delta\gamma_+)^2}^{((\Delta+\Theta_m\gamma_+)^2} \frac{1}{2}\, d\xi_+^2 \frac{\Xi(\xi_-,\xi_+,\varphi)(1-E(\xi_-,\xi_+,\varphi))}{\left[Q^2(\xi_-,\xi_+,\varphi) + (\lambda/R)^2\right]^2}. \tag{19}$$

The angle φ in Eqs. (17)–(21) is the angle between electron and positron momenta in the plane perpendicular to the photon momentum. For small enough angles Δ and Θ_m ($\Delta > \Theta_m$ when the axis of emission cone does not coincide with the crystal axis):

$$|\varphi| \le \varphi_0 = \arctan(\tan\Theta_m/\sin\Delta) \sim \arctan(\Theta_m/\Delta) \sim \Theta_m/\Delta.$$

For those angles φ the pair photoproduction cross-section is small [12] and therefore the most interesting case for an experiment is the case $\Delta = 0$, i.e. the axis of emission cone of e^+e^- pair coincides with the crystal axis. In this geometry, the integration over φ in Eqs. (17)–(19) is performed from 0 up to 2π.

The procedure of integration over an angle φ is similar to described above in Eqs. (8)–(11). After the integration we have:

$$\frac{d\sigma_{coh}}{dx} = N\pi\sigma_0\gamma_+\frac{\lambda}{d}\int_0^{(\Theta_m\gamma_-)^2} d\xi_-^2 \sum_{n=n_1}^{n_2} \Xi(\xi_-,\xi_n,\pi)E(\xi_-,\xi_n,\pi)\Phi(\xi_-,\xi_n)|S(q_\parallel)|^2, \tag{20}$$

$$\frac{d\sigma_{incoh}}{dx} = N\sigma_0\int_0^{(\Theta_m\gamma_-)^2}\frac{1}{2}d\xi_-^2\int_0^{(\Theta_m\gamma_+)^2}\frac{1}{2}d\xi_+^2 \Xi(\xi_-,\xi_+,\varphi)\,(1-E(\xi_-,\xi_+,\varphi))\,\Phi(\xi_-,\xi_+), \tag{21}$$

where the function $\Phi(\xi_-,\xi_n)$ is obtained from Eq. (12) by substitution $\xi_+ \longrightarrow \xi_n$ from Eq. (18). The remaining integration is performed numerically.

3. Numerical results

In order to have an idea about the coherent effect in a thin crystal, Fig. 1a shows the dependence of the differential cross-section (the sum of coherent and incoherent parts)

$$\frac{d\sigma}{d\Theta_-\,d\Theta_+\,d\varepsilon_+} = \frac{d\sigma_{coh}}{d\Theta_-\,d\Theta_+\,d\varepsilon_+} + \frac{d\sigma_{incoh}}{d\Theta_-\,d\Theta_+\,d\varepsilon_+}$$

on the emission angles of electron and positron ($\xi_+ = \gamma_+\Theta_+$, $\xi_- = \gamma_-\Theta_-$), integrated over angle φ between the momenta $\boldsymbol{p}^+$ and $\boldsymbol{p}^-$ in the plane perpendicular to the photon momentum, according to Eqs. (10) and (11), for the case when the photon beam is parallel to the crystal axis consisting of N atoms (symmetrical pairs, $x = \varepsilon_+/\omega = 0.5$ and ⟨100⟩Si crystal) in the vicinity of the coherent peak with $n = 1$ ($\omega = 240$ MeV). Because the cross-section is symmetrical around $\Theta_+ = \Theta_-$, the region $\Theta_+ \leq \Theta_-$ is shown. The cross-section is normalized to the maximum and shows the sharp maximum according to Eqs. (4) and (5).

In order to stress the crystal effect we show in Fig. 1b the maximum values of cross-section $d\sigma/d\Theta_-\,d\Theta_+\,d\varepsilon_+$ of e^+e^- pairs production from amorphous and crystal targets as a function of e^+ emission angle $\xi_+ = \gamma_+\Theta_+$. The procedure of plotting in Fig. 1b is as follows: for given ε_+ energy we calculated $d\sigma/d\Theta_-\,d\Theta_+\,d\varepsilon_+$, and for every given value ξ_+ we find the maximum value of cross-section $d\sigma/d\Theta_-\,d\Theta_+\,d\varepsilon_+$ and plotted in Fig. 1b this value versus ξ_+. Under calculation, Eqs. (10)–(11) for $d\sigma/d\Theta_-\,d\Theta_+\,d\varepsilon_+$ in a crystal was used, and Eq. (16) for $d\sigma_N/d\Theta_-\,d\Theta_+\,d\varepsilon_+$ in an amorphous target was used. The curves are normalized to maximum yield from the crystal

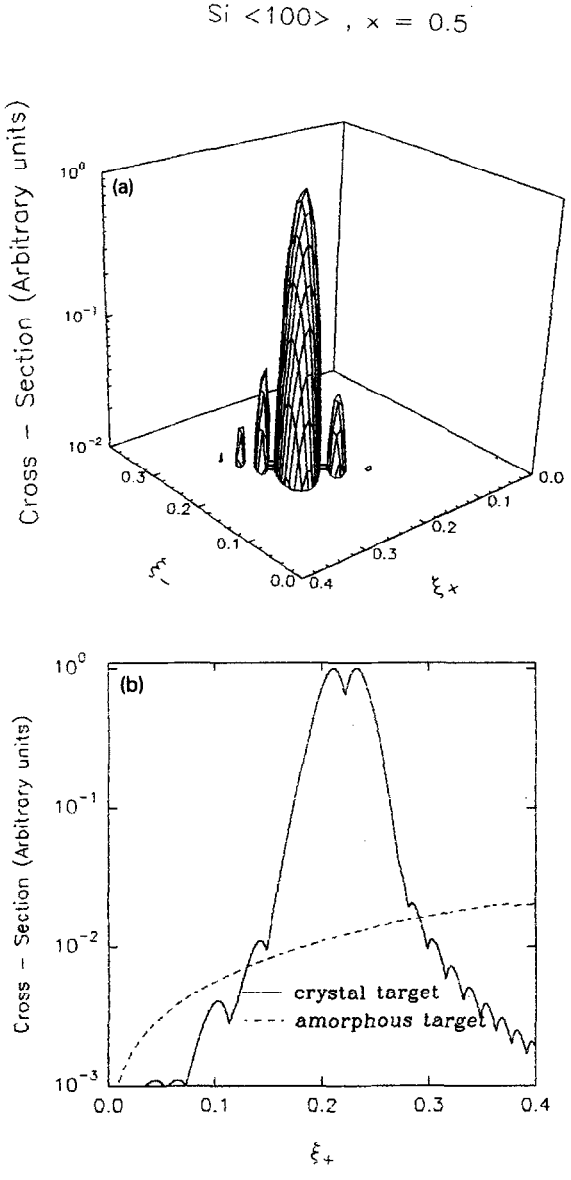

Fig. 1. (a) The dependence of the differential cross-section of type-B pair photoproduction on $\xi_+ = \gamma_+\Theta_+$ and $\xi_- = \gamma_-\Theta_-$ (the sum of coherent and incoherent parts), in the vicinity of the coherent peak $n = 1$, $\omega = 240$ MeV. The target is a Si⟨100⟩ crystal, and the other parameters are: $N = 10^2$, $T = 273$ K, $\gamma_+ = \gamma_- = \omega/2m$. The region $\Theta_+ \leq \Theta_-$ is shown. The cross-section is normalized to the maximum. (b) The curves for maximum cross-section of e^+e^- pairs from amorphous (dashed line) and crystal target (solid line) as a function of e^+ emission angle $\xi_+ = \gamma_+\Theta_+$. The other parameters are the same as in (a). The curves are normalized to the maximum cross-section in the crystal target.

target. Simple analytical estimation shows that the value of deep minimum of the cross-sections in Figs. 1a and 1b, is determined by the factor $m^2/\omega^2 \ll 1$ arising in the differential cross-section (10), (11) and (16) at $\gamma_+\Theta_+ = \gamma_-\Theta_-$. Fig. 1b shows that due to coherence effect, the differential cross-section of pairs production in a thin crystal exceeds

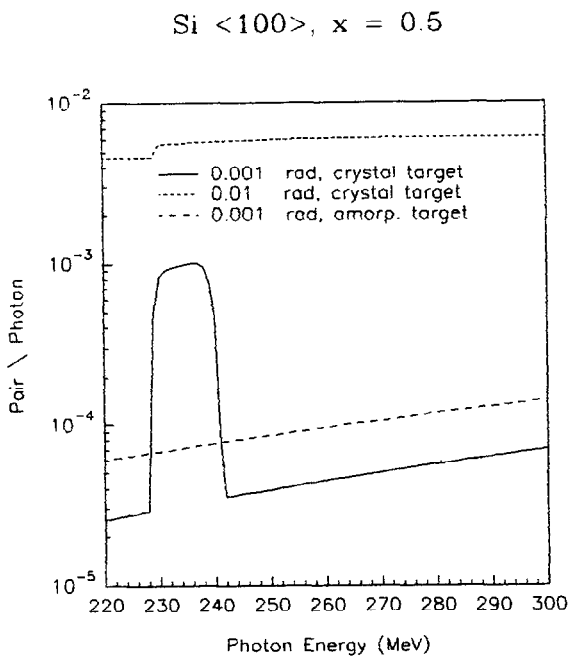

Fig. 2. The yield (the sum of coherent and incoherent parts) of symmetrical e^+e^- pairs under photons interaction with ⟨100⟩Si axis (T = 273 K, L = 0.35 μm), into emission angles cone $\Theta_{m1} \leq 10^{-2}$ (dotted line) and $\Theta_{m2} \leq 10^{-3}$ (solid line). The dashed line represent the cross-section in an amorphous target for the same thickness and into emission angle cone $\Theta_{m2} \leq 10^{-3}$.

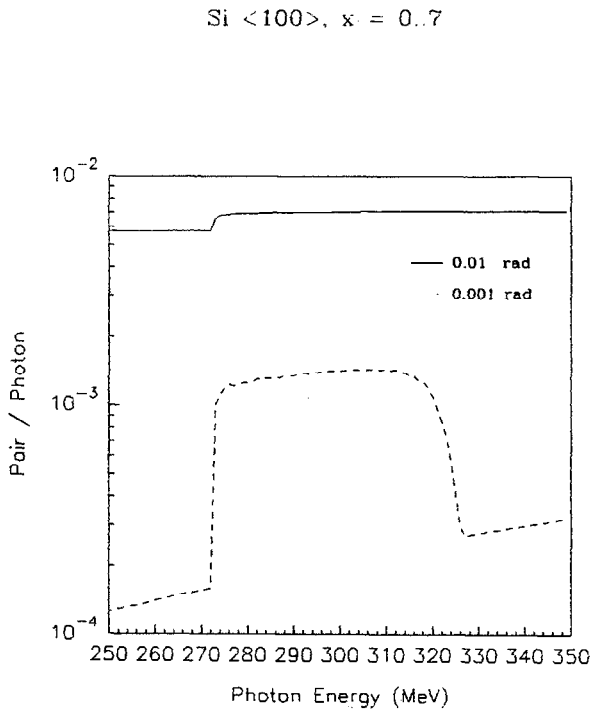

Fig. 3. The yield of asymmetrical e^+e^- pairs (x = 0.7) in dependence on photon energy ω from ⟨100⟩Si axis for two emission angles cone $\Theta_{m1} \leq 10^{-2}$ (dashed line) and $\Theta_{m2} \leq 10^{-3}$ (solid line) (T = 273 K, L = 0.35 μm).

many times the same cross-section in an amorphous target in a definite narrow range of e^+ emission angles.

Let us consider further the photoproduction of equal-energy pairs (symmetrical pairs, $\varepsilon_- = \varepsilon_+ = \hbar\omega/2$; $x = \varepsilon_+/\hbar\omega = 0.5$) with closely the same directions of momenta and the geometry $\Delta = 0$, in the thick crystal. For those pairs, instead of Eq. (5), we can write:

$$\hbar\omega - \frac{cp}{2}(\Theta_+^2 + \Theta_-^2) = g_n, \quad n = 1, 2, 3, \ldots, \tag{22}$$

with $p^+ = p^- = p$.

Fig. 2 shows the results of the calculations according to Eqs. (20) and (21) of the yield of symmetrical pairs in dependence on the photon energy and in the vicinity of the first coherent peak (n = 1, ⟨100⟩Si at the photon energy ω = 240 MeV and crystal thickness L = 0.35 μm), for two values of maximum emission angle $\Theta_{m1} = 10^{-2}$ and $\Theta_{m2} = 10^{-3}$. As it follows from Fig. 2, the coherent peak for Θ_{m2} becomes more brilliant, the maximum value of the peak is of the same order as for Θ_{m1} and the width becomes sufficiently less. The total pair yield for Θ_{m2} decreases in comparison with the case of Θ_{m1} approximately by order of magnitude (mainly due to the suppression of the incoherent part of the cross-section), which one can compensate in an experiment by increase of the bremsstrahlung beam intensity entering the crystal.

Fig. 3 demonstrates the results of the calculation using Eqs. (20) and (21) of the yield of asymmetrical pairs (x = 0.7) for the same kinematics as above in Fig. 2 for symmetrical pairs. The main difference with symmetrical pairs is that the position of coherent peak is shifted, in accordance with Eq. (5), to the region of higher energy photons. The height and the width of coherent peak for the photoproduction of asymmetrical pairs (for given kinematics, $\Delta = 0$) are larger than for the symmetrical pairs.

Therefore, one can investigate the coherent type-B photoproduction of e^+e^- pairs under conditions, when the coherent peak is more brilliant and the incoherent background is suppressed, in an experiment with restricted emission angles of e^+e^- in the final state ("narrow" pair).

4. Coherent photoproduction of relativistic positronium

The partial case of "narrow" pairs (5) production in a crystal is the coherent photoproduction of relativistic positronium atoms [8,9]. The photoproduction of a positronium atom in an amorphous target was first considered in [10,11], where it was shown that the cross-section of positronium photoproduction is proportional to pair photoproduction cross-section with parallel momenta of an electron and positron.

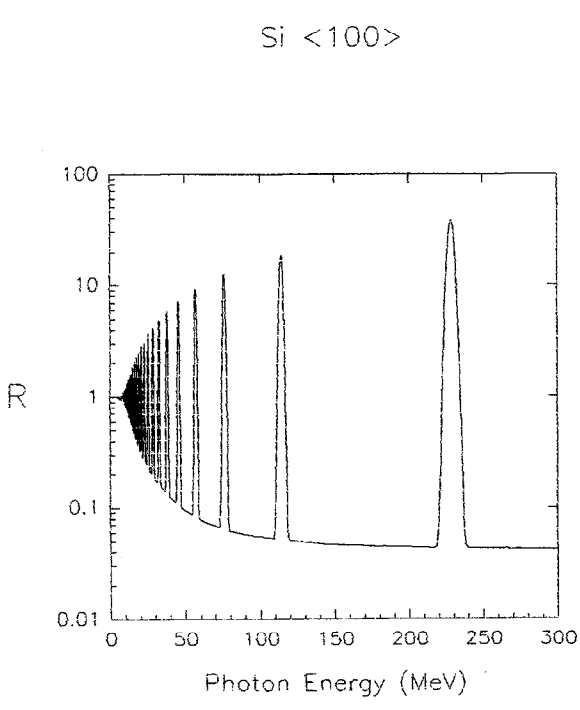

Fig. 4. The relation of the differential cross-sections of photoproduction of positronium atom (bound e^+e^- pair) on the crystal axis consisting of N atoms (Si⟨100⟩, $N = 10^3$, $T = 273$ K) to the same cross-section on N atoms in an amorphous target. The energy spread of incident photon beam $\Delta\omega/\omega = 10^{-2}$ is taken into account.

For the coherent process of type-B in a crystal, the cross-section (in the separate string approximation) has the sharp peaks at the photon energies defined by [8,9]:

$$\omega_n = (4m^2 + g_n^2)/2g_n, \quad n = 1, 2, 3, \ldots, \tag{23}$$

which follows from Eqs. (4) and (5) assuming $\boldsymbol{p}^+ = \boldsymbol{p}^-$.

Fig. 4 shows sharp and large peaks for the ratio

$$R = \frac{\mathrm{d}\sigma_{\mathrm{coh}}(A_{2e}) + \mathrm{d}\sigma_{\mathrm{incoh}}(A_{2e})}{N\,\mathrm{d}\sigma_1(A_{2e})}$$

of the differential cross-section of coherent photoproduction of positronium atom on a separate crystal string consisting of N atoms, to the differential cross-section on N atoms in an amorphous target, calculated according to [8,9], taking into account the energy spread of the initial photon beam $\Delta\omega/\omega = 10^{-2}$. The emission angle of positronium is taken $\theta_{A_{2e}} = \lambda/2\gamma_{A_{2e}}R$, where $\gamma_{A_{2e}}$ is the relativistic factor of a positronium atom ($\theta_{A_{2e}}$ is an angle for which the cross-section $\mathrm{d}\sigma_{\mathrm{coh}}(A_{2e})$ is maximum for given photon energy). Further, the calculations show that the quantity

$$R(\Delta_{A_{2e}}) = \frac{\displaystyle\int_0^{2\pi}\int_0^{\Delta_{A_{2e}}} (\mathrm{d}\sigma_{\mathrm{coh}}(A_{2e}) + \mathrm{d}\sigma_{\mathrm{incoh}}(A_{2e}))\sin\theta\,\mathrm{d}\theta\,\mathrm{d}\varphi}{N\displaystyle\int_0^{2\pi}\int_0^{\Delta_{A_{2e}}} \mathrm{d}\sigma_1(A_{2e})\sin\theta\,\mathrm{d}\theta\,\mathrm{d}\varphi}, \tag{24}$$

which characterizes the increase of the yield in comparison with an amorphous target, as a function of the angular size $\Delta_{A_{2e}}$ of the detector, drops from $R(\Delta_{A_{2e}}) = 34$ at $\Delta_{A_{2e}} = 10^{-4}$ to $R(\Delta_{A_{2e}}) = 17$ at $\Delta_{A_{2e}} = 1 \times 10^{-3}$ and approaches $R(\Delta_{A_{2e}}) = 13.7$ at $\Delta_{A_{2e}} \to \pi$ (for the first resonance peak $n = 1$). The total cross-section of coherent positronium photoproduction is $\sigma_{\mathrm{coh}}(A_{2e}) + \sigma_{\mathrm{incoh}}(A_{2e}) \simeq 8.7$ mb (Si⟨100⟩, $N = 10^3$, $T = 273$ K), for the photon energy $\omega \simeq 229$ MeV near the first coherent peak.

Comparing the enhancement due to the coherence effect under measurements of the total pair yield [6,7], one can see the impressive increase of the coherent peak brilliance (ratio of peak height to background) from $\sim 10^{-1}$ in the case of "usual" pairs up to ~ 10 in the case of "narrow" pairs (Figs. 2 and 3) and up to ~ 10–10^2 in the case of photoproduction of relativistic A_{2e}.

5. Channeling of created particles and position of coherent peak

Similar to the distortion of the shape of the coherent maxima in the type-B coherent bremsstrahlung of the relativistic electrons in a crystal, due to an influence of the interaction of electron with a continuous axial potential [14] one can expect the same effect for the cross-symmetrical process, which is the type-B coherent creation of e^+e^- pairs in a crystal (coherent pair creation in a channeled states).

Let us estimate the typical photon energy region in the vicinity of the coherent peak, where the channeling of pair particles can manifest itself. Let the photon momentum $\boldsymbol{k}$ be parallel to the crystallographic axis. The energy and longitudinal momentum conservations can be written as:

$$\omega = \sqrt{(p_\parallel^+)^2 + m^2} + \sqrt{(p_\parallel^-)^2 + m^2} + \varepsilon_\perp^+ + \varepsilon_\perp^-, \tag{25}$$

$$\boldsymbol{k} = \boldsymbol{p}_\parallel^+ + \boldsymbol{p}_\parallel^- + \boldsymbol{g}_n, \qquad |\boldsymbol{k}| = \omega, \tag{26}$$

where g_n is defined in Section 2 and $\varepsilon_\perp^+$, $\varepsilon_\perp^-$ are so called transverse energies of the positron and the electron in a continuous potential of a crystallographic axis. These energies and the corresponding wave functions are the eigenvalues and the eigen wave functions of the corresponding quantum equation describing channeling of the electron (positron) in a crystal (see, for the relativistic particles channeling e.g. the review [15]).

Let us further introduce new definition for the symmetrical pairs: $p_{\parallel}^{-} = p_{\parallel}^{+} = p$. Using this definition and substituting p from Eq. (26) into Eq. (25) we obtain after simple algebra:

$$\omega_n^* = \frac{4m^2 + g_n^2 + \Delta_\perp^2}{2g_n} \frac{1}{(1 - \Delta_\perp/g_n)}, \tag{27}$$

where $\Delta_\perp = \varepsilon_\perp^+ + \varepsilon_\perp^-$ characterizes the channeling of the created particles of pair. The case $\Delta_\perp = 0$ corresponds to the coherent pair creation without taking into account the interaction of e^+e^- with the continuous axial potential and leads to the formula for the threshold for appearance of a coherent peak

$$\omega_n^* = \omega_n = (4m^2 + g_n^2)/2g_n, \quad n = 1, 2, 3, \ldots,$$

which coincides with the positions of the coherent maxima exactly as in the standard (without channeling) theory [1–5], see also Section 2. Of course, if we take into account the term $p_\perp^2/2m$ for above barrier motion, the position of a peak shifts towards a large ω value.

As it follows from Eq. (27), the interactions of e^+e^- with a continuous axial potential lead to the "spread" of the threshold for appearance of the coherent maximum. In order to estimate the "uncertainty" of position of the coherent peak it is enough to substitute $\Delta_\perp = \pm V_0$, where V_0 is the characteristic value of the depth of axial potential well. In particular, in Section 3 we calculated the position of coherent peak ($n = 1$) for type-B pair photoproduction in ⟨100⟩Si at ($\omega_1 = 240$ MeV). For this case $g_1 = 2\pi/d \sim 2.3$ MeV, $V_0 \sim 140$ eV, i.e. $\Delta_\perp/g_1 \sim 0.08$, which leads to the uncertainty of the peak position $\Delta\omega_1 \sim \pm 15$ MeV near the one obtained using standard theory value $\omega_1 = 240$ MeV.

Thus, for the coherent type-B pair photoproduction we can expect the change of the shape of the coherent peak in the region of about 30 MeV near $\omega_1 = 240$ MeV, due to the interaction of the pair particles with an axial continuous potential. Our Eq. (27) estimates only the photon energy region where the channeling of created particles can change the shape of coherent peaks. In order to describe the shape of the coherent peak quantitatively, one has to leave the standard theory of coherent pair creation [1–5] and to carry out the calculation of a matrix elements using not plane waves but wave functions of particles which are solutions of the corresponding wave equations with a continuous axial potential. As one can suppose, the greater the $\Delta_\perp$ value is, the less will be the matrix element since it depends strongly on the overlapping of electron and positron wave functions in a classically forbidden (for each of the particles) region, which strongly depends on a transverse energies of created particles.

The effect of the "spread" of the position of coherent peak depends on the crystal temperature T due to a dependence of V_0 on T. We found from Eq. (27) an additional temperature shift of the position of the coherent peak caused by the temperature decrease from T_1 to T_2:

$$\omega_n^*(T_2) - \omega_n^*(T_1) = \omega_n \frac{[V_0(T_2) - V_0(T_1)]/2\pi d}{[1 - V_0(T_1)/2\pi d][1 - V_0(T_1)/2\pi d]}. \tag{28}$$

For example, the typical amplitude of a change of $V_0(T)$ for the case of ⟨100⟩Si is: $V_0(300\text{ K}) = 140$ eV, $V_0(0\text{ K}) \sim 175$ eV, i.e. the maximum additional uncertainty of the position of coherent peak can be about ~10 MeV and therefore the total "uncertainty" at $T = 0$ K can reach the value ~40 MeV near the photon energy about $\omega = 240$ MeV, defined using the standard coherent theory.

The estimation of the channeling effect on the coherent creation of asymmetrical pairs can be done in a similar way as by obtaining of the formula (27) but the algebra is more complicated.

Since the height of coherent maxima is proportional to the Debye–Waller factor $\exp(-q^2\bar{u}^2)$ (see Eq. (2)), which increases with the temperature decrease, there appear two effects: the first one is the increase of the height of the coherent peak and the second one is the increase of the width of this peak.

Thus, the channeling of created particles can change the brilliance of coherent peaks as compared with our numerical results, see Figs. 2 and 3. The experimental investigation of type-B coherent pair photoproduction in a channeled states (including temperature effect) could be very interesting, but requires more fine experimental resolution as used before [7].

6. Conclusion

In conclusion, we point out that:

1. The simple estimation shows that the channeling of created pair particles can lead to the uncertainty of the position of coherent peak and probably to the splitting of coherent peak which is the combined effect of quantum electrodynamics analogous to the splitting of the peak in the coherent bremsstrahlung of type-B [14]. Therefore, the special kinematics described above (when the coherent peak is more brilliant and the incoherent background is suppressed) is favourable for the experimental investigations of the structure of coherent peaks and for the search of combined effects. An interesting observation is that the magnitude of the combined effect depends on the crystal temperature according to Eq. (28).

2. The experimental studies of the influence of correlations between electron and positron momenta in the final states can be considered as the first stage of the sequential transition to an experiment which is the observation of the coherent photoproduction of positronium atoms in a crystal [8,9] and the search for the Sakharov effect [13].

3. The increase of the relative height of the coherent peak and the suppression of the incoherent background under the special kinematics for type-B photoproduction can be considered as a possible method to prepare a positron (elec-

tron) beam with a small angular and energy spread and particles energies 10^2–10^3 MeV. The advantages of the crystal target in comparison with an amorphous target are: i) the photoproduction cross-section in a crystal has narrow maxima at definite photon energies and positron emission angles; ii) the yield of positrons from the crystal target at some given values of Θ_m and ε_+ is greater in terms of orders of magnitude in comparison to the yield from amorphous target, see Figs. 2 and 3. The necessary position of coherent peak (which defines the positron energy) can be chosen by changing the type of a crystal or (and) type of the crystal axis or by changing the x value. The production of intense positron beams using the channeling radiation from the crystal target plus a conversion of this radiation into pairs in an amorphous target has been discussed recently in [16,17], but this methods is valid for production of positrons with rather wide energy spectrum ranging from 10 to 50 MeV.

4. The possibility discussed above of the increase of brilliance of coherent peaks can be applied not only for the type-B photoproduction of e^+e^- pairs but for an arbitrary direction of the photon momentum with respect to the crystal axis (the type-A process). In this case all three components of momentum transferred to the crystal are quantized and our relation (4) is replaced by three equations which connect the incident photon energy with energies and momenta of the created electron and positron. In this case the typical photon energies at which the coherent peaks appear are much greater than for the type-B process considered here.

Acknowledgements

The authors thank V.N. Zabaev and M.Yu. Andreyashkin for useful discussions. One of authors (Yu.L.P.) was partially supported by Russian State Scientific-Technical Program "Fundamental Nuclear Physics", Contract 135-09. One of the authors (Yu.P.K.) wishes to thank Prof. H.A. Olsen for fruitful discussions and The Institute of Physics, University of Trondheim, where the work was completed, for warm hospitality extended to him.

References

[1] M.L. Ter-Mikaelian, High-Energy Electromagnetic Processes in Condensed Media (Wiley-Interscience, New York, 1972).
[2] H. Uberall, Phys. Rev. 103 (1956) 1055.
[3] G. Diambrini-Palazzi, Rev. Mod. Phys. 10 (1968) 611.
[4] N. Cue and J.C. Kimball, Phys. Lett. A 124 (1987) 191.
[5] S.M. Darbinian, K.A. Ispirian, A.T. Margarian, Preprint EPhI-1007(58)-87, 1987, Erevan.
[6] R.O. Avakyan, A.E. Avetisyan, V.A. Gurdjan, K.R. Dallakyan, S.S. Danagulian, S.M. Darbinian, K.A. Ispirian, O.S. Kizogian, A.T. Margarian, Yu.Z. Susiasian, S.P. Taroyan, Pis'ma Zh. Eksk. Teor. Fiz. 51 No. 7 (1990) 627 (JETP Lett. 51 (1990) 396).
[7] M.Yu. Andreyashkin, A.Yu. Basai, S.A. Vorobiev, V.N. Zabaev, B.N. Kalinin, Yu.P. Kunashenko, Yu.L. Pivovarov, Pis'ma Zh. Eksp. Teor. Fiz. 55 No. 7 (1992) 407 (JETP Lett. 55 No. 7 (1992) 413).
[8] Yu.P. Kunashenko and Yu.L. Pivovarov, Yad. Fiz. 51 (1990) 627 (Sov. J. Nucl. Phys. 51(3) (1990) 397).
[9] Yu.P. Kunashenko and Yu.L. Pivovarov, Izv. Akad. Nauk. Ser. Fiz. 57 No. 1 (1993) 156 (Bull. Russian Acad. Sci. Phys. 57 (1) (1993) 144.
[10] H.A. Olsen, Phys. Rev. D 33 No 7 (1986) 2033.
[11] V.L. Luboshits, Yad. Fiz. 45 (1987) 1099 (Sov. J. Nucl. Phys. 45 (1987) 682).
[12] V.B. Berestetskii, E.M. Lifshitz, L.P. Pitaevskii, Quantum Electrodynamics (Nauka, Moscow, 1980; in russian).
[13] A.D. Sakharov, Zh. Eksp. Teor. Fiz. 18 (1948) 631.
[14] K.Yu. Amosov, B.N. Kalinin, G.A. Naumenko, A.P. Potylitsin, V.P. Sarytchev, Pis'ma Zh. Exp. Teor. Fiz. 55 No. 10 (1992) 587 (JETP Lett., 55 No. 10 (1992) 612).
[15] N. Cue and J.C. Kimball, Phys. Reports 125 (1985) 70.
[16] R. Chehab, F. Conhot, A.R. Nagiesh, F. Richard, X. Artru, LAP RT 89-01 or PAC, Chicago, 1989.
[17] F.J. Pecker, SLAC-PUP-5482, 1991.